

THE STRESS FIELD AND ENERGY OF A THREE-DIMENSIONAL DISLOCATION LOOP AT A CRACK TIP

PETER M. ANDERSON* and JAMES R. RICE

Division of Applied Sciences, Harvard University, Cambridge, MA 02138, U.S.A.

(Received 16 February 1987)

ABSTRACT

THE SELF STRESS field and self energy are estimated for a planar 3D dislocation loop emanating from a half-plane crack tip. While the problem is of greatest interest for analysis of shear loops nucleating from the crack tip in the concentrated stress field there due to applied loadings, it is addressed here in the interest of tractability for 3D prismatic loops lying in the same plane as the crack. Exact elastic calculations for that case are based on recent developments of 3D crack weight function theory and specific results are given for induced stress fields, intensity factors and energy of semicircular and rectangular prismatic dislocation loops. Also, self stresses and energy expressions are derived for the 2D case of a line dislocation lying parallel to the crack for arbitrary Burgers vector type and general orientation of the dislocated plane relative to the crack plane, and those results are used together with the 3D prismatic loop results to estimate approximately the self energy for 3D shear dislocation loops emanating from the tip on planes inclined to the crack plane. Energy results are given in terms of a correction factor m to the usual estimate of energy for an emergent crack tip loop as half the energy of a full loop (identified as the emergent loop and its image relative to the crack tip) in an uncracked solid. That is, if the energy of a full circular loop of radius r in an uncracked solid is $2\pi r A_0 \ln(8r/e^2 r_0)$, with r_0 = core cut-off and A_0 = energy factor, then the energy of a semicircular loop of radius r emerging from the crack tip is shown to take the form $\pi r A_0 \ln(8mr/e^2 r_0)$ and the constant m is calculated here as 2.2 for a prismatic loop ahead of a crack and estimated approximately to range from about 1.2 to 1.9 for representative shear loops inclined to the crack plane. The self energy exceeds the half-full-loop value, corresponding to $m = 1$, and it is observed that this effect increases by \sqrt{m} the predicted loads to nucleate a dislocation loop of the assumed shape from a crack tip.

1. INTRODUCTION

WE PRESENT here calculations of the stress field and self energy for a dislocation loop emerging from a crack tip. The problem is of interest mainly for shear dislocations, in estimating when they may be nucleated from the tip by the concentration of an applied stress field there, and arises also in the study of whether a solid may be regarded as intrinsically cleavable (e.g., RICE and THOMSON, 1974; MASON, 1979; OHR, 1985; LIN and THOMSON, 1986; ANDERSON, 1986; ANDERSON, and RICE, 1986). However an exact calculation, within continuum elastic dislocation theory, of the stress field and self energy of a 3D loop at a crack tip has not previously appeared.

* Current address: Engineering Department, Trumpington St., Cambridge University, Cambridge CB2 1PZ, U.K.

the problem is difficult in general but a reasonably tractable version of it is in the form of a prismatic (opening) dislocation loop emerging from the crack tip and lying on the same plane as the crack. That case is analyzed here and detailed results are given for the special cases of semicircular and rectangular loops.

To understand the nature of a principal result, let us recall that the elastic self energy of a full circular dislocation loop of radius r in an infinite uncracked solid has the form (HIRTH and LOTHE, 1968)

$$U^{\text{full loop}} = 2\pi r A_0 \ln(8r/e^2 r_0), \quad (1.1)$$

where r_0 is the core cut-off radius and, for a prismatic loop of opening Burgers displacement b in an isotropic solid,

$$A_0 = \mu b^2 / 4\pi(1 - \nu) \quad (1.2)$$

(μ = shear modulus, ν = Poisson ratio). As SCATTERGOOD (1980) and BACON *et al.* (1979) show, the same form as in equation (1.1) holds for a circular loop of arbitrary Burgers vector and with general elastic anisotropy, with A_0 being the average around the circle of the quantity $b_\alpha A_{\alpha\beta} b_\beta$ in equation (2.3) to follow. By comparison, we show here (Section 5) that the self energy of a semi-circular prismatic loop of radius r emerging from the crack tip on the same plane as the crack has the form

$$U = \pi r A_0 \ln(8mr/e^2 r_0), \quad (1.3)$$

where the constant $m \approx 2.2$. RICE and THOMSON (1974) approximated the energy U of a general semicircular loop emerging from the crack tip by the above form with $m = 1$, i.e. by estimating U as half the energy of a full circular loop, motivated by their exact 2D result for the force on a near tip dislocation as we discuss subsequently. When the prismatic dislocation loop ahead of the crack is highly elongated in the direction along the crack front, so that its stress field effectively reduces to the 2D field of a straight prismatic dislocation lying parallel to the tip, we find here that the analogously defined $m = 2$. In fact, the 2D crack-dislocation problem can be analyzed for arbitrary Burgers vectors and arbitrary orientation angle ϕ of the dislocated surface relative to the tip using well-known elastic solutions as summarized recently by LIN and THOMSON (1986). In this way we show (Section 6) for the 2D problem that when the dislocated surface lies in the plane of the crack, $\phi = 0$, the analogously defined $m = 2$ independent of the Burgers vector type, but that m decreases with ϕ according to a relation that is different for each of the cases of prismatic, edge-type shear and screw-type shear Burgers vectors.

By combining our 3D results for prismatic dislocations on $\phi = 0$ and 2D results for arbitrary Burgers vector and arbitrary ϕ , we propose (Section 7) an approximate estimate of the energy correction factor m for general 3D shear dislocation loops of semicircular shape emanating from a crack tip and find that for representative cases of tensile loaded cracks in f.c.c. crystals and bicrystals m lies between approximately 1.2 and 1.9. As may be seen from equation (1.3), the insertion of the factor m into the self energy is the equivalent of altering the core size from r_0 to r_0/m in the type of loop nucleation calculations done by MASON (1979) and ANDERSON and RICE (1986). Since $m > 1$, this is equivalent to a decrease of the effective core size (i.e. to an increase of core energy) and shows up as an increase in the predicted load to nucleate a

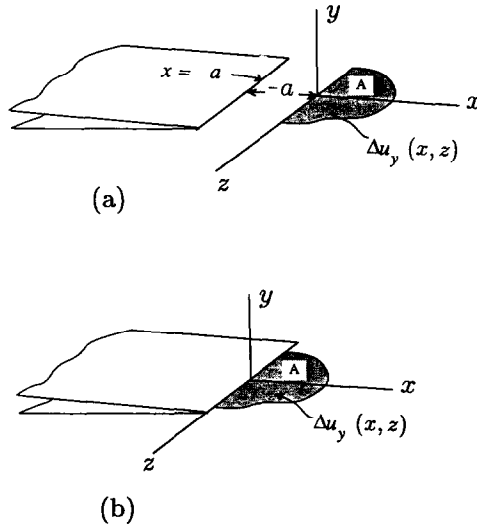


FIG. 1. (a) Prismatic dislocation over area A ahead of crack with tip at $x = a$ (negative a is shown). (b) Prismatic loop emanating from crack tip at $x = 0$.

dislocation by comparison to the case when the m effect is disregarded and U is approximated as half the full loop energy. The predicted crack tip stress intensity factor necessary for nucleation is increased by \sqrt{m} , i.e. by 10 to 40% in typical cases. Such effects are discussed by ANDERSON (1986).

2. BACKGROUND FOR 3D CRACK-DISLOCATION CALCULATIONS

The background for our 3D calculations of Sections 3 to 5, to follow, is given in two recent papers by RICE (1985a, b) on 3D weight function theory. To examine this formulation for a half-plane crack in an infinite elastic solid, let the crack lie on the plane $y = 0$ with tip parallel to the z -axis along the line $x = a$, such that the region $x < a$ is cracked (e.g. Fig. 1a, where the a shown is negative).

Let us first recall that general external loadings induce a singularity at the crack tip such that stress components σ_{ij} (indices i, j, k, l range over Cartesian directions x, y, z here) ahead of the tip on $y = 0$ vary as

$$[\sigma_{yy}, \sigma_{yx}, \sigma_{yz}] \sim [K_1, K_2, K_3]/\sqrt{2\pi(x-a)}. \tag{2.1}$$

The stress intensity factors K_α (indices α, β range over 1, 2, 3) so defined may vary with position z along the crack front and appear also in the expression

$$G = K_\alpha \Lambda_{\alpha\beta} K_\beta \tag{2.2}$$

for the crack tip energy release rate. Following anisotropic elastic crack theory (STROH, 1958; BARNETT and ASARO, 1972), the coefficients $\Lambda_{\alpha\beta} = (1/8\pi)A_{\alpha\beta}^{-1}$ where $A_{\alpha\beta}^{-1}$ is the inverse of the prelogarithmic energy factor matrix $A_{\alpha\beta}$ appearing in the expression

$$\hat{U} = b_x A_{x\beta} b_\beta \ln (r_1/r_0) \quad (2.3)$$

(r_1 = outer cut-off radius) for the energy per unit length of a straight dislocation line lying parallel to the z -axis in an uncracked solid; here, when the dislocated plane adjoining the dislocation line is of type $y = \text{constant}$, $b_1 = b_y$ is the prismatic opening, $b_2 = b_x$ is the in-plane or edge-type shear, and $b_3 = b_z$ is the anti-plane or screw-type shear component of Burgers vector. For the isotropic solid, $\Lambda_{x\beta}$ is diagonal with

$$\Lambda_{11} = \Lambda_{22} = (1-\nu)/2\mu, \quad \Lambda_{33} = 1/2\mu. \quad (2.4)$$

RICE (1985a) showed that three vector "weight functions"

$$\mathbf{h}_\alpha = \mathbf{h}_\alpha(x-a, y, z-z'), \quad \alpha = 1, 2, 3,$$

associated with the three crack tip stress intensity modes and having Cartesian components h_{ai} , may be defined for the cracked configuration and have the following properties. First, when the cracked solid is loaded by arbitrary body force components $f_i(x, y, z)$ per unit volume, the intensity factors induced at location z' along the crack front are given by

$$K_\alpha(z') = \iiint h_{ai}(x-a, y, z-z') f_i(x, y, z) dx dy dz, \quad (2.5)$$

where the integral extends over all loaded regions. Second, when in the presence of a fixed system of applied loads the crack front position is changed from the straight line $x = a$ to the curved position $x = a + \varepsilon g(z)$, the initial rate of change with ε of the displacement field $u_i = u_i(x, y, z; \varepsilon)$ is

$$[\partial u_i(x, y, z; \varepsilon)/\partial \varepsilon]_{\varepsilon=0} = 2\Lambda_{x\beta} \int_{-\infty}^{+\infty} h_{ai}(x-a, y, z-z') K_\beta(z') g(z') dz'. \quad (2.6)$$

where $K_\beta(z)$ is the intensity factor distribution induced by the fixed set of applied loads. Note that when $g(z) = 1$, equation (2.6) gives $\partial u_i(x, y, z; a)/\partial a$. RICE (1985a, equations (58)–(60)) derived the half-plane crack weight function field \mathbf{h}_1 for an isotropic solid, by using equation (2.6) as its defining property, and gave expressions for \mathbf{h}_2 and \mathbf{h}_3 as some formidable and as yet unevaluated double integrals. The function \mathbf{h}_1 can also be obtained by further analysis of results by BUECKNER (1977) for tensile mode fields that vary as $\cos(\lambda z)$ along the crack front, and BUECKNER (1987) independently derived closed-form results for all three \mathbf{h}_α , again for the isotropic solid.

The above concepts were applied by RICE (1985b) to represent the self stress fields and stress intensity factor distributions induced by general 3D dislocation loops in unbounded solids with half-plane cracks. He observed that the mechanical effects of arbitrary distributions of Eshelby transformation strain can be represented as the response to an appropriate field of body force f_i in equation (2.5), and noted that a general Somigliana displacement discontinuity $\Delta \mathbf{u} = \mathbf{u}^+ - \mathbf{u}^-$ on surface A , having normal \mathbf{N} pointing from the $(-)$ to the $(+)$ sides of A , can be represented as a transformation strain distribution which is Dirac singular on A (e.g. Fig. 1a for the prismatic loop case). In this way RICE (1985b) derived the result

$$K_x(z') = \iint_A h_{xi,i}(x-a, y, z-z') C_{ijkl} N_k(x, y, z) \Delta u_l(x, y, z) dA(x, y, z) \quad (2.7)$$

for the intensity factor distributions induced by the dislocation. Here C_{ijkl} is the modulus tensor with the usual symmetries and $\Delta \mathbf{u}$ and \mathbf{N} are defined for points (x, y, z) on A . While not mentioned explicitly by RICE as a limitation, it has been noted by T. L. SHAM (private communication, 1986) that the integral in equation (2.7) is not well defined when the crack tip lies in or along the border of the dislocated surface A . Unfortunately, such is the case of interest for an emergent loop at the crack tip, and we show how to deal with that situation in the next section for the specific case of a prismatic loop ahead of the crack tip.

Equation (2.7) defines $K_x(z)$, which is now also to be recognized as a function of crack tip position a . To acknowledge such we write it as $K_x(z, a)$ in the next equation. By setting $g = 1$ in property (2.6) above for the weight functions and then integrating on a from $a = -\infty$ to $a = 0$, we obtain

$$u'_i(x, y, z) \equiv u_i(x, y, z) - u_i^0(x, y, z) = 2\Lambda_{\alpha\beta} \int_{-\infty}^0 \int_{-\infty}^{+\infty} h_{xi}(x-a, y, z-z') K_\beta(z', a) dz' da \quad (2.8)$$

for the displacement. Here \mathbf{u} is the displacement field induced by the dislocation loop in presence of the half-plane crack with tip at $x = 0$, as in Fig. 1b and \mathbf{u}^0 is the displacement field induced by the same loop in an infinite uncracked solid. From the last result and stress-strain relations we may evaluate the stress components in the form $\sigma'_{ij} \equiv \sigma_{ij}(x, y, z) - \sigma_{ij}^0(x, y, z)$, where σ_{ij} is the dislocation self stress field in the presence of the crack and σ_{ij}^0 is the same for the uncracked solid.

This synopsis shows how to evaluate the field of an arbitrary 3D dislocation loop near a crack and, at least for the isotropic solid, all the requisite weight functions are now available. The calculations are most readily addressed for the prismatic loop ahead of the crack since that requires knowledge only of $\mathbf{h}_1(x, y, z)$ which is of simpler form than \mathbf{h}_2 and \mathbf{h}_3 .

3. PRISMATIC DISLOCATION DISTRIBUTION AT A CRACK TIP

As shown in Fig. 1b, the prismatic loop lies in the crack plane, $y = 0$, and is described by an arbitrary distribution of displacement discontinuity, $\Delta u_y(x, z) = u_y(x, 0^+, z) - u_y(x, 0^-, z)$ normal to the crack plane. Here the dislocation displacement $\Delta u_y(x, z)$ is assumed to remain nonzero, in general, as x approaches the crack tip (i.e. that $\Delta u_y(0^+, z)$ is nonzero).

The self stress distribution, $\sigma_{yy}(x, 0, z)$, is expressed as an addition σ'_{yy} to the self stress field σ_{yy}^0 for the same loop in an uncracked body, so that

$$\sigma_{yy}(x, 0, z) = \sigma_{yy}^0(x, 0, z) + \sigma'_{yy}(x, 0, z), \quad (3.1)$$

where (RICE, 1986b, equation (54))

$$\sigma'_{yy}(x, 0, z) = \frac{\mu}{2\pi^2(1-\nu)} \int_{-\infty}^{+\infty} \int_0^{+\infty} \frac{1}{D^3} \left[\frac{D}{2\sqrt{x\bar{x}}} - \arctan \frac{D}{2\sqrt{x\bar{x}}} \right] \Delta u_y(\bar{x}, \bar{z}) \, d\bar{x} \, d\bar{z}, \tag{3.2}$$

with

$$D = \sqrt{(x-\bar{x})^2 + (z-\bar{z})^2}.$$

It is noted that the integrand in equation (3.2) is bounded for values (\bar{x}, \bar{z}) which approach (x, z) when $x > 0$. Also, σ_{yy}^0 produced by the prismatic loop in an infinite, uncracked body with same coordinates is (e.g., RICE, 1986b, equation (59))

$$\sigma_{yy}^0(x, 0, z) = \frac{\mu}{4\pi^2(1-\nu)} \int_{-\infty}^{+\infty} \int_0^{+\infty} \left[\frac{(\bar{x}-x)}{D^3} \frac{\partial}{\partial \bar{x}} + \frac{(\bar{z}-z)}{D^3} \frac{\partial}{\partial \bar{z}} \right] \Delta u_y(\bar{x}, \bar{z}) \, d\bar{x} \, d\bar{z}, \tag{3.3}$$

with the understanding that $\Delta u_y(\bar{x}, \bar{z})$ may be nonzero only for $\bar{x} \geq 0$ (and hence that $\partial u_y(\bar{x}, \bar{z})/\partial \bar{x}$ will be Dirac singular at $\bar{x} = 0$ when $\Delta u_y(0^+, \bar{z}) \neq 0$). Each of the expressions $\sigma'_{yy}, \sigma_{yy}^0$ have singularities which behave as $1/x$ in distance from the crack front. However, those contributions from the terms cancel when their sum is taken. A square root singularity, $1/\sqrt{x}$, remains in $\sigma_{yy}(x, 0, z)$ and defines $K_1(z)$ as discussed.

The means by which the $1/x$ singularity terms are isolated and combined is first to show that $\sigma_{yy}(x, 0, z) = 0$ for the case of a prismatic dislocation of uniform Burgers vector \mathbf{b} situated on the plane $y = 0$ ahead of the crack and over the area $-\infty < z < +\infty, 0 \leq x < +\infty$. This simply describes a uniform jacking up of the ligament ahead of the crack, so that $\sigma_{yy}(x, 0, z) = 0$ is expected, yet $\sigma_{yy}^0(x, 0, z)$ and $\sigma'_{yy}(x, 0, z)$ will individually contain $1/x$ singularities. In particular, this geometry describes a straight dislocation line situated on the z -axis, and $\sigma_{yy}^0(x, 0, z)$ is then known from elementary dislocation theory and may be calculated from equation (3.3) as

$$\sigma_{yy}^0 = -\frac{\mu b}{2\pi(1-\nu)x}. \tag{3.4}$$

The corresponding value of $\sigma'_{yy}(x, 0, z)$ for the case of a uniform displacement discontinuity b ahead of the crack is evaluated by setting $\Delta u_y(\bar{x}, 0, \bar{z}) = b$ in equation (3.2), in which case it may be shown that

$$\sigma'_{yy} = \frac{\mu b}{2\pi(1-\nu)x}. \tag{3.5}$$

Thus, in anticipation of combining $1/x$ singularities as just observed, but for the general case, equation (3.2) for $\sigma'_{yy}(x, 0, z)$ is rearranged by separating out a term due to a uniform displacement, $\Delta u_y(\hat{x}, \hat{z})$, analogous to the form in equation (3.5), so that

$$\begin{aligned} \sigma'_{yy}(x, 0, z) &= \frac{\mu \Delta u_y(\hat{x}, \hat{z})}{2\pi(1-\nu)x} \\ &+ \frac{\mu}{2\pi^2(1-\nu)} \int_{-\infty}^{+\infty} \int_0^{+\infty} \frac{1}{D^3} \left[\frac{D}{2\sqrt{x\bar{x}}} - \arctan \frac{D}{2\sqrt{x\bar{x}}} \right] [\Delta u_y(\bar{x}, \bar{z}) - \Delta u_y(\hat{x}, \hat{z})] \, d\bar{x} \, d\bar{z}. \end{aligned} \tag{3.6}$$

For present purposes, we regard the choice of (\hat{x}, \hat{z}) as arbitrary, although we will shortly wish to choose it as $(0^+, z)$.

To factor out the $1/x$ singularity in the expression for $\sigma_{yy}^0(x, 0, z)$, the contribution to the integral in \bar{x} between 0^- and 0^+ is evaluated, noting that over this ‘‘strip’’, $\partial u_y(\bar{x}, \bar{z})/\partial \bar{x} = \Delta u_y(0^+, \bar{z})\delta(\bar{x})$. The result is given as

$$\begin{aligned} \sigma_{yy}^0(x, 0, z) = & -\frac{\mu}{4\pi(1-\nu)} \int_{-\infty}^{+\infty} \frac{x\Delta u_y(0^+, \bar{z}) d\bar{z}}{[x^2 + (z - \bar{z})^2]^{3/2}} \\ & + \frac{\mu}{4\pi(1-\nu)} \int_{-\infty}^{+\infty} \int_{0^+}^{+\infty} \left(\frac{\bar{x} - x}{D^3} \frac{\partial}{\partial \bar{x}} + \frac{\bar{z} - z}{D^3} \frac{\partial}{\partial \bar{z}} \right) \Delta u_y(\bar{x}, \bar{z}) d\bar{x} d\bar{z}. \end{aligned} \quad (3.7)$$

The first integral contains the $1/x$ contribution to $\sigma_{yy}^0(x, 0, z)$. For example, if $\Delta u_y(x, z) = b$ for $x \geq 0$ and $-\infty < z < \infty$ is chosen as discussed earlier, the first integral in equation (3.7) provides the only contribution, equal to that given in equation (3.4), by noting

$$\int_{-\infty}^{+\infty} \frac{x d\bar{z}}{[x^2 + (z - \bar{z})^2]^{3/2}} = \frac{2}{x}. \quad (3.8)$$

Equations (3.6) and (3.7), which represent $\sigma'_{yy}(x, 0, z)$ and $\sigma_{yy}^0(x, 0, z)$, are added to form $\sigma_{yy}(x, 0, z)$. The first two terms of both equations each provide $1/x$ contributions, which are combined by choosing $(\hat{x}, \hat{z}) = (0^+, z)$ in equation (3.6). In addition, equation (3.8) is used so that

$$\begin{aligned} \sigma_{yy}(x, 0, z) = & -\frac{\mu x}{4\pi(1-\nu)} \int_{-\infty}^{+\infty} \frac{\Delta u_y(0^+, \bar{z}) - \Delta u_y(0^+, z)}{[x^2 + (z - \bar{z})^2]^{3/2}} d\bar{z} \\ & + \frac{\mu}{2\pi^2(1-\nu)} \int_{-\infty}^{+\infty} \int_0^{+\infty} \frac{\Delta u_y(\bar{x}, \bar{z}) - \Delta u_y(0^+, z)}{D^3} \left[\frac{D}{2\sqrt{x\bar{x}}} - \arctan \frac{D}{2\sqrt{x\bar{x}}} \right] d\bar{x} d\bar{z} \\ & + \frac{\mu}{4\pi(1-\nu)} \int_{-\infty}^{+\infty} \int_{0^+}^{+\infty} \left(\frac{\bar{x} - x}{D^3} \frac{\partial}{\partial \bar{x}} + \frac{\bar{z} - z}{D^3} \frac{\partial}{\partial \bar{z}} \right) \Delta u_y(\bar{x}, \bar{z}) d\bar{x} d\bar{z}. \end{aligned} \quad (3.9)$$

This result provides the stress induced for arbitrary opening $\Delta u_y(x, z)$. The choice $(\hat{x}, \hat{z}) = (0^+, \bar{z})$ assures that the first integral remains finite as x approaches zero, at least at values of z for which $\Delta u_y(0^+, z)$ is suitably continuous. The term in the second integral which behaves as $1/2D^2\sqrt{x\bar{x}}$ now provides the only singular contribution as x approaches zero, and behaves as $\sim 1/\sqrt{x}$. The mode 1 stress intensity factor is now obtained in a straightforward manner from equations (2.1) and (3.9) as

$$\begin{aligned} K_I(z) = & \lim_{x \rightarrow 0^+} \sqrt{2\pi x} \sigma_{yy}(x, 0, z) \\ = & \frac{\mu}{(2\pi)^{3/2}(1-\nu)} \int_{-\infty}^{+\infty} \int_0^{+\infty} \frac{\Delta u_y(\bar{x}, \bar{z}) - \Delta u_y(0^+, z)}{\sqrt{\bar{x}[\bar{x}^2 + (\bar{z} - z)^2]}} d\bar{x} d\bar{z}. \end{aligned} \quad (3.10)$$

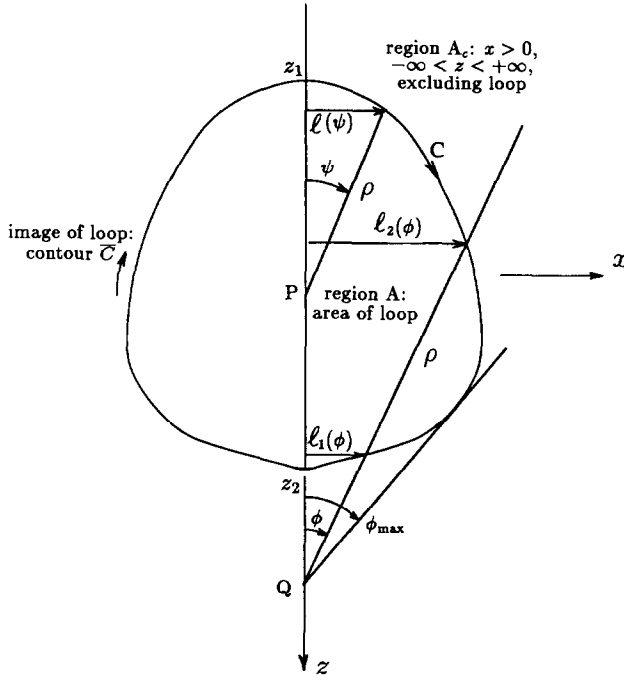


FIG. 2. Integration path and coordinates for an arbitrarily shaped prismatic loop.

This corresponds to equation (34) of RICE (1986b), as a special case of equation (2.7) above, except that now an additional term $\Delta u_y(0^+, z)$ appears in the integrand, allowing consideration of opening dislocations for which $\Delta u_y(0^+, z) \neq 0$, and the integral extends even over points $(\bar{x}, 0, \bar{z})$ ahead of the crack where $\Delta u_y(\bar{x}, \bar{z}) = 0$. The integral without that additional term is divergent, as suggested in the discussion following equation (2.7). When A in equation (2.7) is planar and the crack tip lies in A or along one of its borders, it is evident from consideration of the null self stress of a uniformly dislocated half-plane emanating from the crack tip that a similar fix-up can be applied in general to equation (2.7): we can calculate the induced intensity factors by replacing $\Delta \mathbf{u}(x, y, z)$ in equation (2.7) by $\Delta \mathbf{u}(x, y, z) - \Delta \mathbf{u}(a, 0, z)$ and extending the integration over the entire half-plane (or pair of half-planes, when the tip divides A into two parts) in which A resides.

4. RESULTS FOR K_I INDUCED BY UNIFORM BURGERS VECTOR IN PRISMATIC LOOP

Here, equation (3.10) is applied to obtain $K_I(z)$ induced along a straight crack front by an arbitrarily shaped prismatic loop with *uniform* Burgers vector \mathbf{b} , situated directly ahead of and in the plane of the crack. The results are then specialized for semicircular and rectangular shapes. Figure 2 shows the relevant geometry for the arbitrarily shaped loop, in which A denotes the area of the loop and A_c denotes the region of the crack plane $x > 0$, $-\infty < z < +\infty$, but excluding A .

Different expressions for $K_1(z)$ result when the observation point z is inside or outside A . In the case where the observation position lies inside the loop, as denoted by point P in Fig. 2, $\Delta u_y(\bar{x}, \bar{z}) - \Delta u_y(0, z)$ is zero in the loop area A and equals $-b$ in the area A_c outside of it. If the observation point lies outside of the loop, as denoted by point Q , then $\Delta u_y(\bar{x}, \bar{z}) - \Delta u_y(0, z) = b$ inside the loop and is zero outside. Thus, equation (3.10) is restated for the particular cases as

$$\begin{aligned}
 K_1(z) &= -\frac{\mu b}{(2\pi)^{3/2}(1-\nu)} \int_{A_c} \frac{d\bar{x} d\bar{z}}{\sqrt{\bar{x}} [\bar{x}^2 + (z-\bar{z})^2]} \quad (z \text{ inside } A), \\
 &= \frac{\mu b}{(2\pi)^{3/2}(1-\nu)} \int_A \frac{d\bar{x} d\bar{z}}{\sqrt{\bar{x}} [\bar{x}^2 + (z-\bar{z})^2]} \quad (z \text{ outside } A).
 \end{aligned}
 \tag{4.1}$$

The area integrals can be expressed in polar coordinates centered about the observation point z , and are depicted in Fig. 2 as (ρ, ψ) for a point P inside the loop, and as (ρ, ϕ) for a point Q outside the loop. After integration in ρ the results take on a rather simple form,

$$K_1(P) = -\frac{\mu b}{\sqrt{2\pi}(1-\nu)} \frac{1}{\pi} \int_0^\pi \frac{d\psi}{\sqrt{l(\psi)}} \quad (z_P \text{ inside } A), \tag{4.2}$$

$$K_1(Q) = \frac{\mu b}{\sqrt{2\pi}(1-\nu)} \frac{1}{\pi} \int_0^{\phi_{\max}} \left(\frac{1}{\sqrt{l_1(\phi)}} - \frac{1}{\sqrt{l_2(\phi)}} \right) d\phi \quad (z_Q \text{ outside } A). \tag{4.3}$$

Here, $l(\psi)$, $l_1(\phi)$, $l_2(\phi)$ are the perpendicular distances from the crack front to integration points along the perimeter of the dislocation loop, as shown in Fig. 2. It is seen here for positive b that K_1 is negative along the crack front inside the loop (e.g. at point P), but it is positive elsewhere along the crack front (e.g. at point Q).

The integral expression for $K_1(P)$ in equation (4.2) is simply the average of $1/\sqrt{l(\psi)}$ over the loop perimeter; in the case of a straight dislocation line, we obtain the 2D result,

$$K_1^{2D} = -\frac{\mu b}{\sqrt{2\pi l}(1-\nu)}, \tag{4.4}$$

as derived by RICE and THOMSON (1974). This observation suggests an approximation for the general 3D case which is exact for the loop geometry discussed here, namely that at a point P inside the loop, the mode α stress intensity factor is

$$K_\alpha^{3D}(P) = \frac{1}{\pi} \int_0^\pi K_\alpha^{2D}(\psi) d\psi, \tag{4.5}$$

where K_α^{2D} in equation (4.5) is the factor for a 2D straight dislocation line of the same Burgers vector sitting at distance $l(\psi)$ from the crack front.

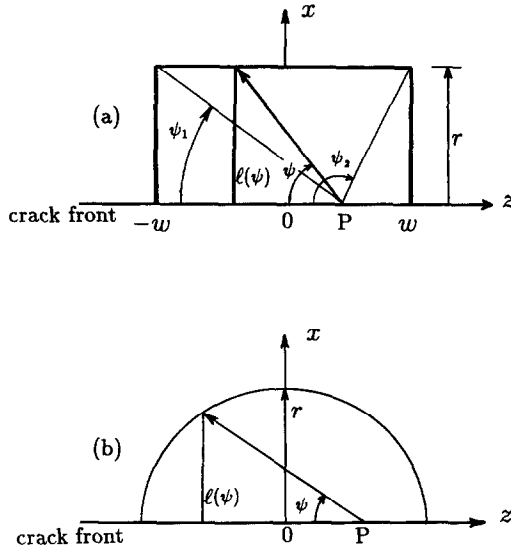


FIG. 3. Geometries for (a) rectangular and (b) semicircular loops, showing coordinates and angles used to evaluate equation (4.2) for $K_1(z)$.

$K_1(z)$ may be determined for a point P inside a rectangular shaped loop of dimension $2w$ by r shown in Fig. 3a. Equation (4.2) is applied by defining $l(\psi)$ as shown in Fig. 3a, and integrating around the perimeter of the loop, to obtain

$$K_1(z) = - \frac{\mu b}{(1-\nu)\sqrt{2\pi r}} \times \left[\frac{\psi_2 - \psi_1}{\pi} + \frac{1}{\pi} \int_0^{\psi_1} \sqrt{\frac{\tan \psi_1}{\tan \psi}} d\psi + \frac{1}{\pi} \int_{\psi_2}^{\pi} \sqrt{\frac{\tan(\pi - \psi_2)}{\tan(\pi - \psi)}} d\psi \right] \quad (z \text{ inside rect. loop}), \quad (4.6)$$

where ψ_1 and ψ_2 describe the position of the observation point z along the crack front according to $\tan \psi_1 = r/(w+z)$, $\tan(\pi - \psi_2) = r/(w-z)$.

In a similar manner, equation (4.2) is specialized to the case of a semicircular loop of radius r , defining $l(\psi)$ as shown in Fig. 3b,

$$K_1(z) = - \frac{\mu b}{(1-\nu)\sqrt{2\pi r}} \frac{1}{\pi} \int_0^{\pi} \frac{[1 + (z/r) \cos \phi]}{[1 + 2(z/r) \cos \phi + (z/r)^2] \sqrt{\sin \phi}} d\phi \quad (z \text{ inside semicircular loop}). \quad (4.7)$$

Presented in Figs. 4 and 5 are the values of $K_1(z)$ induced by rectangular and semicircular prismatic loops, respectively. In the former, several values of aspect ratio, r/w , are chosen to examine the effect of loop geometry on K_1 . A comparison of the result for $r/w = 1$ to that for the semicircle shows very good agreement, with the magnitude of K_1 marginally higher in the latter case. Near the corners of the loop along the crack front, $K_1(z)$ behaves as the inverse square root of distance from the

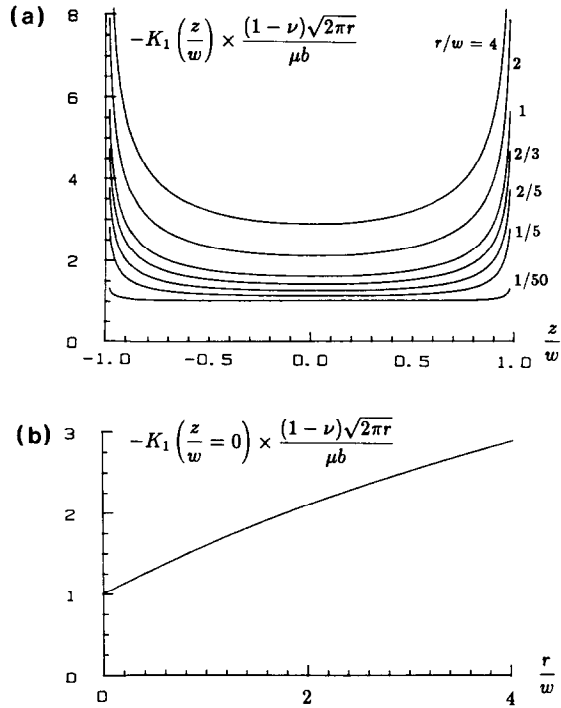


FIG. 4. Values of K_1 inside rectangular loops, (a) as a function of aspect ratio r/w and position z/w along the crack front and (b) at the center of the crack front as a function of r/w .

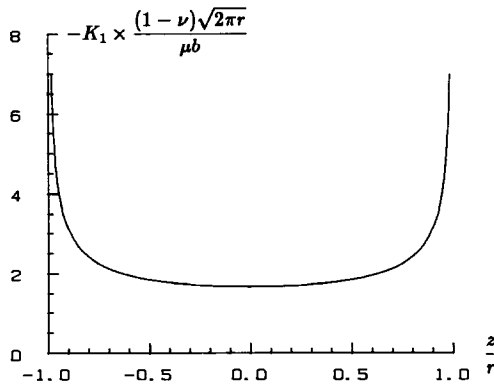


FIG. 5. Values of K_1 for semicircular loops as a function of position z/r along the crack front.

corner. As the aspect ratio of the loop is increased, these corner effects penetrate toward the center and elevate K_1 along the entire crack front. It is seen for the case of $r/w = 1/50$ that corner effects are negligible over most of the crack front, and $K_1 = -\mu b / (1-\nu) \sqrt{2\pi r}$, the known value for a straight dislocation line. Also shown in Fig. 4 is K_1 at the center of the rectangular loop as a function of the aspect ratio. $-K_1(z/w = 0)$ increases continuously with r/w . For dislocation loop aspect ratios

less than 1 (i.e. less than that of a semicircle), $-K_1$ ranges between 1 and $1.6 \times \mu b / (1-\nu) \sqrt{2\pi r}$.

The effects of shielding the crack tip from applied load are predicted to be higher along the entire crack front in the 3D loop geometry as compared to the 2D case. The level of shielding in the loop shapes considered here is minimum at the center, and increases steadily as one moves toward a corner of the loop. Given that the crack front is uniform, without stress concentrators or different levels of crack tip blunting within the loop, the most likely location in the loop for future dislocation nucleation or crack extension would appear to be at the loop center, where the shielding is a minimum. Irregularly shaped loops which deviate from a semicircular or rectangular shape would favor a location which is most "distant" from the loop perimeter, in the sense of averaging $1/l(\psi)$ around the loop, as shown in equation (4.2).

5. THE STRESS DISTRIBUTION AND SELF ENERGY OF A CRACK TIP PRISMATIC DISLOCATION LOOP

We now calculate the energy to introduce an arbitrarily shaped prismatic dislocation loop into an unloaded, but cracked body. As in Section 4, the dislocation loop is situated on the crack plane and has ends at the crack front. The energy is expressed in terms of one-half the self energy of the corresponding "full loop" in an infinite, uncracked body, plus a correction term which we identify here. The full loop is constructed as the crack tip loop, plus a reflected image about the crack front. Thus, the full loop representation of the dislocation depicted in Fig. 2 is given by the loop enclosed by contours C and \bar{C} . The energy difference represented by the correction will be seen to be independent of an elastic core cutoff parameter used in dislocation theory.

The development begins with calculation of the difference in stress, $\sigma_{yy}(x, 0, z) - \sigma_{yy}^{\text{full loop}}(x, 0, z)$. The difference in energy will then be calculated by integration of this stress difference times the work conjugate b over the area of the loop. Note that $\sigma_{yy}^{\text{full loop}}$, the stress induced by the full loop in an infinite uncracked body, is not the same as σ_{yy}^0 ; the latter corresponds to the stress induced by the half on $x > 0$ of what we now call the full loop. Also, the stress σ_{yy} for the prismatic loop is unbounded as inverse distance from the perimeter of the loop, and as inverse square root of distance from the crack front. In integrating over the loop to obtain elastic strain energy, the presence of the former singularity requires an elastic core cutoff for the dislocation to be chosen so as to keep energy bounded. Here, the choice of a core cutoff is avoided by calculating the difference in stress, $\sigma_{yy}(x, 0, z) - \sigma_{yy}^{\text{full loop}}(x, 0, z)$, between the exact elastic result and that for the full dislocation loop in an infinite body. Using equation (3.3), $\sigma_{yy}(x, 0, z)$ for a full prismatic dislocation loop of uniform b in an infinite body is written as

$$\sigma_{yy}^{\text{full loop}}(x, 0, z) = -\frac{\mu b}{4\pi(1-\nu)} \int_{C+\bar{C}} \left[\frac{(\bar{x}-x) d\bar{z} - (\bar{z}-z) d\bar{x}}{D^3} \right], \quad (5.1)$$

where the contours C and \bar{C} define the perimeter of the loop and its image about the crack front, in a clockwise sense as shown in Fig. 2.

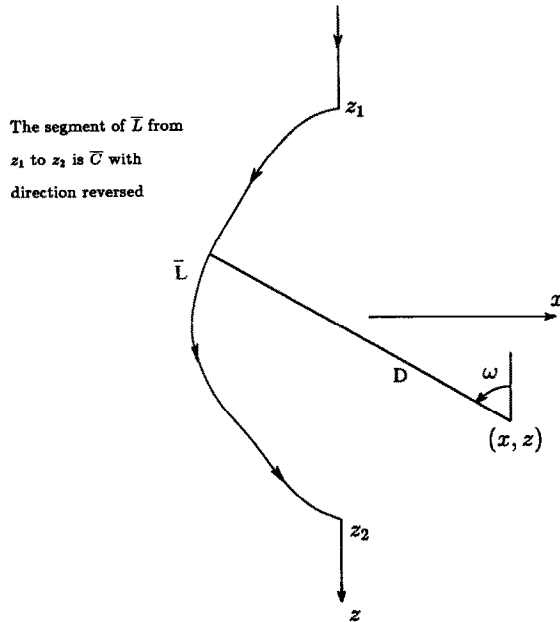


FIG. 6. Integration contour \bar{L} used in the evaluation of equation (5.2).

The difference in stress, $\sigma_{yy}(x, 0, z) - \sigma_{yy}^{\text{full loop}}(x, 0, z)$, at a point within the loop is obtained by evaluating equation (3.9) for $\sigma_{yy}(x, 0, z)$, and setting $\Delta u_y(x, z) = b$ within the loop area A . The integrand of the first term does not contribute when $\Delta u_y(0^+, \bar{z}) = \Delta u_y(0^+, z)$, or equivalently, when the location \bar{z} is within the loop. For similar reasons, the second term contributes only in the area domain A_c , and the third term equals the contribution to $\sigma_{yy}^{\text{full loop}}(x, 0, z)$ in equation (5.1) from the path C . Thus, the third term is written as $\sigma_{yy}^{\text{full loop}}(x, 0, z)$ minus the integral over \bar{C} in equation (5.1), to obtain

$$\begin{aligned}
 [\sigma_{yy}(x, 0, z) - \sigma_{yy}^{\text{full loop}}(x, 0, z)] &= \frac{\mu b x}{4\pi(1-\nu)} \left(\int_{-\infty}^{z_1} + \int_{z_2}^{+\infty} \right) \\
 &\times \frac{d\bar{z}}{[x^2 + (\bar{z} - z)^2]^{3/2}} + \frac{\mu b}{4\pi(1-\nu)} \int_C \frac{(\bar{x} - x) d\bar{z} - (\bar{z} - z) d\bar{x}}{D^3} \\
 &\quad - \frac{\mu b}{2\pi^2(1-\nu)} \int_{A_c} \left(\frac{D}{2\sqrt{x\bar{x}}} - \arctan \frac{D}{2\sqrt{x\bar{x}}} \right) \frac{d\bar{x} d\bar{z}}{D^3}. \quad (5.2)
 \end{aligned}$$

Here, z_1 and z_2 are the boundaries of the uniform prismatic loop along the crack front, and A_c is defined as earlier (see Fig. 2).

The first two integrals in equation (5.2) reduce to a line integral over the contour \bar{L} shown in Fig. 6, of the quantity $d\omega/D$, where ω is the angular coordinate (in the form of rotation about the y -axis) and D the distance from the observation point to

the integration point along \bar{L} . The result for a uniform prismatic loop of arbitrary shape is given as

$$\begin{aligned}
 [\sigma_{yy}(x, 0, z) - \sigma_{yy}^{\text{full loop}}(x, 0, z)] = & \frac{\mu b}{4\pi(1-\nu)} \left[\frac{1 - (z - z_1)/\sqrt{x^2 + (z - z_1)^2}}{x} \right. \\
 & + \frac{1 + (z - z_2)/\sqrt{x^2 + (z - z_2)^2}}{x} - \int_c \frac{d\omega}{D} \\
 & \left. - \frac{2}{\pi} \int_{A_c} \left(\frac{D}{2\sqrt{x\bar{x}}} - \arctan \frac{D}{2\sqrt{x\bar{x}}} \right) \frac{d\bar{x} d\bar{z}}{D^3} \right], \quad (5.3)
 \end{aligned}$$

where the first two terms represent contributions from the parts of the contour \bar{L} from $-\infty$ to z_1 and z_2 to ∞ , respectively. These terms are not singular along the z -axis (i.e., when $x = 0$), except when z approaches z_1 or z_2 as well. In the vicinity of the corners, $(\sigma_{yy} - \sigma_{yy}^{\text{full loop}}) \sim 1/(\text{distance from the corner})$, but this singularity provides a finite contribution to the energy difference to be calculated. Along the crack front, the first term in the integral over A_c provides an inverse square root dependence of $\sigma_{yy}(x, 0, z) - \sigma_{yy}^{\text{full loop}}(x, 0, z)$ on x , representing the K_1 that is induced at the crack tip by the prismatic loop, and again providing only a finite contribution to the energy difference.

5.1. Specialization to semicircular geometry and stress distribution on dislocated surface

For the case of a semicircular loop of radius r , equation (5.3) may be stated as

$$\begin{aligned}
 [\sigma_{yy}(x, 0, z) - \sigma_{yy}^{\text{full loop}}(x, 0, z)] \times \left[\frac{-4\pi(1-\nu)r}{\mu b} \right] = & \frac{2}{\pi} \int_{-\pi/2}^{+\pi/2} \int_0^1 \frac{\Lambda - \arctan \Lambda}{M} d\eta d\theta \\
 & - \frac{1 - (z+r)/\sqrt{x^2 + (z+r)^2}}{x/r} - \frac{1 - (r-z)/\sqrt{x^2 + (r-z)^2}}{x/r} \\
 & - \int_0^\pi \frac{[1 + (x \sin \phi + z \cos \phi)/r] d\phi}{[1 + 2(x \sin \phi + z \cos \phi)/r + (x^2 + z^2)/r^2]^{3/2}}, \quad (5.4)
 \end{aligned}$$

where

$$\Lambda = \frac{1}{2} \left[\frac{1 - 2\eta(x \cos \theta + z \cos \theta)/r + \eta^2(x^2 + z^2)/r^2}{\eta(x/r) \cos \theta} \right]^{1/2}$$

and

$$M = \left[1 + \eta^2 \frac{x^2 + z^2}{r^2} - 2\eta \frac{x \cos \theta + z \sin \theta}{r} \right]^{3/2}.$$

Figures 7 and 8 present the circumferential and radial plots, respectively, of $[\sigma_{yy}(x, 0, z) - \sigma_{yy}^{\text{full loop}}(x, 0, z)]$ in units of $[-\mu b/4\pi(1-\nu)r]$. The stresses associated with a prismatic opening loop are compressive, and the figures show that higher compressive stresses arise in the crack tip prismatic loop than in the full loop in an infinite,

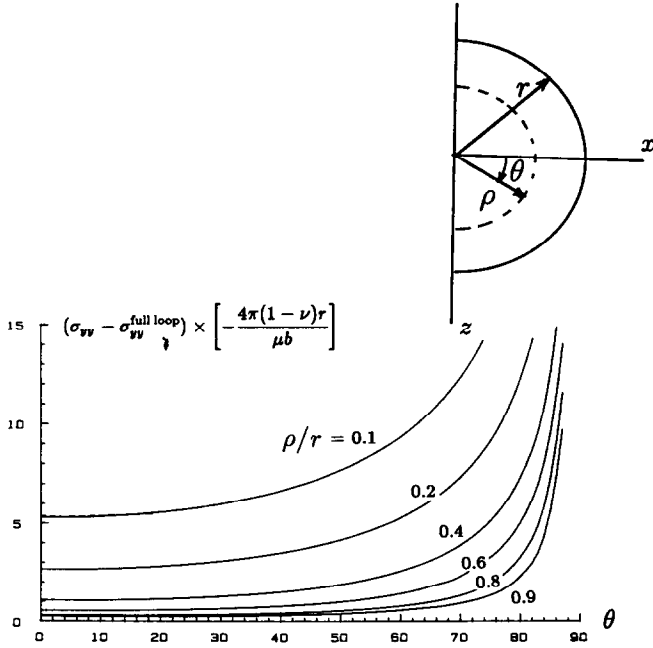


FIG. 7. Circumferential plot of $\sigma_{yy}(x, 0, z) - \sigma_{yy}^{\text{full loop}}(x, 0, z)$ for semicircular prismatic loop of radius r as a function of radial distance ρ and angle θ .

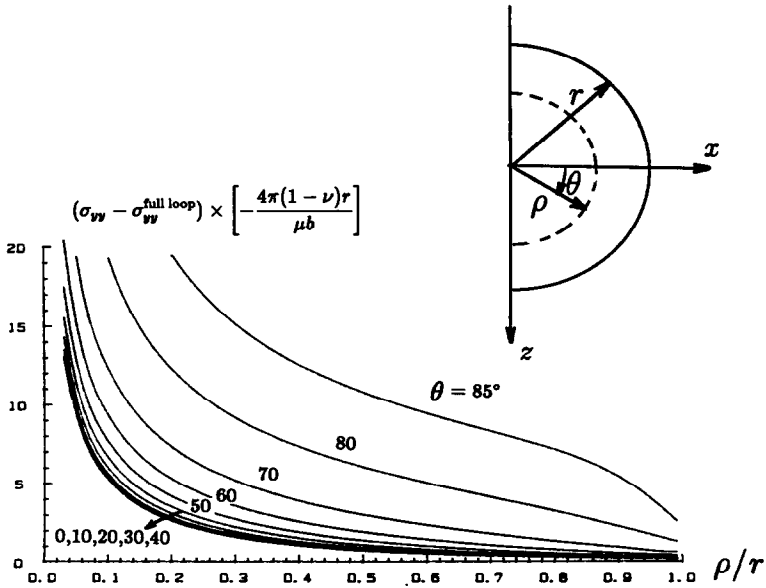


FIG. 8. Radial plot of $\sigma_{yy}(x, 0, z) - \sigma_{yy}^{\text{full loop}}(x, 0, z)$ for semicircular prismatic loop of radius r as a function of radial distance ρ and angle θ .

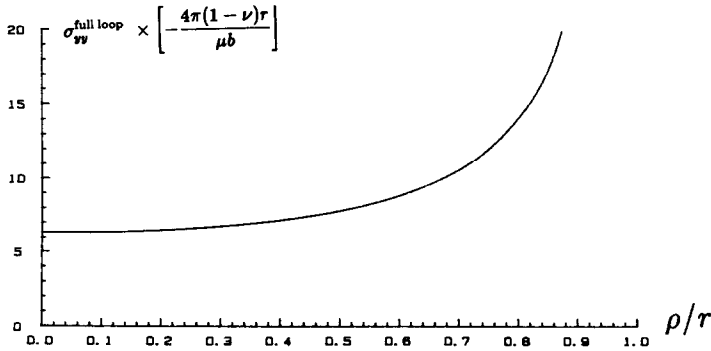


FIG. 9. Radial plot of $\sigma_{yy}^{\text{full loop}}(x, 0, z)$ for circular prismatic loop of radius r as a function of radial distance ρ from loop center.

uncracked body. Compared to the full loop case where $\sigma_{yy}(x, 0, z)$ is uniform along a circumferential path, σ_{yy} along the circumferential paths shown in Fig. 7 is made nonuniform at least in part by the inverse square root dependence on distance from the crack tip. Thus, along such a path, the smallest compressive stresses are situated at $\theta = 0^\circ$ and increase monotonically as θ approaches 90° .

In studies of dislocation nucleation, the radial "force" acting on each segment of the dislocation is obtained from the Peach-Koehler relation, and in the present case is a "climb" force. Thus, the equilibrium position is given from summing contributions from the K -field, due to applied loadings, that due to the self field of the full loop in an uncracked solid, and that represented here in Figs. 7 and 8 as $\sigma_{yy} - \sigma_{yy}^{\text{full loop}}$.

The stress $\sigma_{yy}^{\text{full loop}}(x, 0, z)$ for a prismatic circular loop in an infinite, uncracked body is presented in Fig. 9. The total stress field of the crack tip prismatic loop is given by the sum of $[\sigma_{yy}(x, 0, z) - \sigma_{yy}^{\text{full loop}}(x, 0, z)]$ presented in Figs. 7 and 8 with $\sigma_{yy}^{\text{full loop}}(x, 0, z)$. The latter has an inverse distance dependence as ρ/r approaches 1, which is of opposite sign and stronger than the inverse distance dependence of $[\sigma_{yy}(x, 0, z) - \sigma_{yy}^{\text{full loop}}(x, 0, z)]$ at the loop corners near the crack. Thus, $\sigma_{yy}(x, 0, z)$ is negative with inverse distance dependence from the dislocation loop corners. This agrees with dependence of K_1 on the inverse square root of distance from the crack tip (see Fig. 5).

5.2. Energy and correction factor m for a semicircular shape

The difference in elastic energy between the crack tip prismatic dislocation loop and one half that of the corresponding full loop in an infinite, uncracked body is calculated by integrating $-(b/2)[\sigma_{yy}(x, 0, z) - \sigma_{yy}^{\text{full loop}}(x, 0, z)]$ over the entire crack tip loop on $x > 0$. Although the stress difference is unbounded along the crack front, the energy difference is bounded, and this is independent of a (small) dislocation core cutoff parameter. This feature allows the energy for the semicircular loop to be expressed in terms of one-half the corresponding full loop energy (see equation (1.1)), plus a correction term used to define quantity $\ln m$,

$$U = \pi r A_0 \ln \frac{8r}{e^2 r_0} + \pi r A_0 \ln m = \pi r A_0 \ln \frac{8mr}{e^2 r_0}. \tag{5.5}$$

Thus, m is defined by

$$U - \frac{1}{2} U^{\text{full loop}} = -\frac{b}{2} \int_A [\sigma_{yy}(x, 0, z) - \sigma_{yy}^{\text{full loop}}(x, 0, z)] dA = \pi r A_0 \ln m. \tag{5.6}$$

Evaluation of the integral in equation (5.6) for the semicircular prismatic dislocation loop of Burgers vector b , lying on the crack plane in an isotropic material yields $m \approx 2.21$. As will be seen in Section 6, this value is somewhat higher than an analogously defined m calculated for a 2D crack-dislocation line geometry, which ranges from 2 for when the crack and loop plane are coplanar as in the geometry here, to between 1.1 and 1.4 for when the loop and crack plane are perpendicular. The latter range is given since m in general depends on the dislocation character (except when the crack and slip planes are coplanar) as well as the orientation of the crack and slip planes.

5.3. Stress field, energy and correction factor m for rectangular shape

Similarly, one may determine the difference in stress, $[\sigma_{yy}(x, 0, z) - \sigma_{yy}^{\text{full loop}}(x, 0, z)]$, for a rectangular, prismatic loop of dimension $2w$ parallel to and r perpendicular to the crack front (see Fig. 3). Using equation (5.3), and setting $z_1 = -w, z_2 = +w$,

$$\begin{aligned} \sigma_{yy}(x, 0, z) - \sigma_{yy}^{\text{full loop}}(x, 0, z) &= \sigma_{yy}^{\bar{L}}(x, 0, z) \\ &- \frac{\mu b}{4\pi(1-\nu)} \left[\frac{2}{\pi} \int_{A_c} \left(\frac{D}{2\sqrt{x\bar{x}}} - \arctan \frac{D}{2\sqrt{x\bar{x}}} \right) \frac{d\bar{x} d\bar{z}}{D^3} \right], \end{aligned} \tag{5.7}$$

where D and A_c are defined as earlier, and where $\sigma_{yy}^{\bar{L}}$ is the contribution from the first three terms in equation (5.3) which represent the integration over contour \bar{L} , and may be expressed as (for simplicity, the notation $x' = x/r$ and $z' = z/w$ is used here)

$$\begin{aligned} \sigma_{yy}^{\bar{L}} \times \left[\frac{4\pi(1-\nu)r}{\mu b} \right] &= \frac{1}{x'} \left(1 - \frac{1+z'}{\sqrt{(x'r/w)^2 + (1+z')^2}} \right) \\ &+ \frac{r/w}{1+z'} \left(\frac{(1+x')r/w}{\sqrt{((1+x')r/w)^2 + (1+z')^2}} - \frac{x'r/w}{\sqrt{(x'r/w)^2 + (1+z')^2}} \right) \\ &+ \frac{1}{1+x'} \left(\frac{1+z'}{\sqrt{((1+x')r/w)^2 + (1+z')^2}} - \frac{z'-1}{\sqrt{((1+x')r/w)^2 + (z'-1)^2}} \right) \\ &+ \frac{r/w}{(z'-1)} \left(\frac{x'r/w}{\sqrt{(x'r/w)^2 + (z'-1)^2}} - \frac{(1+x')r/w}{\sqrt{((1+x')r/w)^2 + (z'-1)^2}} \right) \\ &+ \frac{1}{x'} \left(\frac{(z'-1)}{\sqrt{(x'r/w)^2 + (z'-1)^2}} + 1 \right). \end{aligned} \tag{5.8}$$

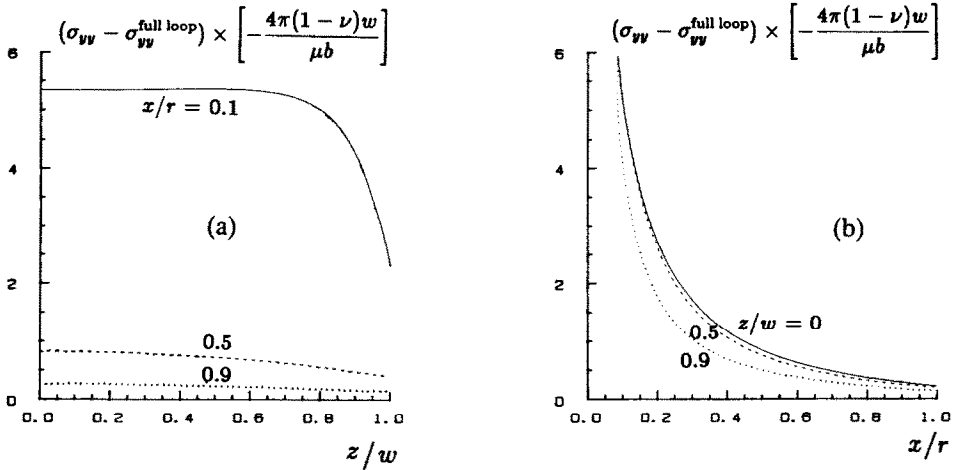


FIG. 10. Profiles of the difference in stress, $\sigma_{yy}(x, 0, z) - \sigma_{yy}^{\text{full loop}}(x, 0, z)$, for a rectangular prismatic dislocation loop of aspect ratio $r/w = 1$, where r and $2w$ denote the loop dimensions perpendicular and parallel, respectively, to the crack front (see Fig. 3a). Results shown for (a) constant $x/r = 0.1, 0.5, 0.9$, and (b) constant $z/w = 0, 0.5, 0.9$.

All terms in the expression for σ_{yy}^L are bounded within the rectangular loop, except at the corners along the crack front, where $\sigma_{yy}^L \sim 1/\text{distance}$ from the corner. The integral over A_c in equation (5.7) is bounded throughout the loop, except along the crack front, where $\sigma_{yy} \sim 1/\sqrt{x}$. Figure 10 presents for $r/w = 1$ profiles of $(\sigma_{yy} - \sigma_{yy}^{\text{full loop}})$ for either constant x or z within the loop. The constant x profiles display the $1/\text{distance}$ singularity at the corner $x = 0, z = w$. The field is symmetric in z , so that $\sigma_{yy}(x, z) = \sigma_{yy}(x, -z)$. The constant z profiles clearly display the $1/\sqrt{x}$ singularity, and show the bounded nature of the stress field as $x \rightarrow r$.

The difference in elastic energy of the crack tip loop and one-half that of the corresponding full loop is expressed similarly in terms of the factor m . Thus, the self energy of a rectangular loop of dimension r perpendicular to the crack front, by $2w$ along the crack front is given as

$$U = 2(w+r)A_0 \left[\ln \frac{2m\sqrt{rw}}{r_0} + f(r/w) \right], \tag{5.9}$$

where

$$f(r/w) = \frac{1}{1+(r/w)} \left[\ln \frac{2\sqrt{r/w}}{1+[1+(r/w)^2]^{1/2}} + (r/w) \ln \frac{2\sqrt{r/w}}{(r/w)+[1+(r/w)^2]^{1/2}} \right] + 2 \frac{[1+(r/w)^2]^{1/2}}{1+(r/w)} - 1,$$

so that setting $m = 1$ produces one-half the energy of a full rectangular prismatic loop of dimension $2r$ by $2w$ in an infinite uncracked body. Thus, m is evaluated according to

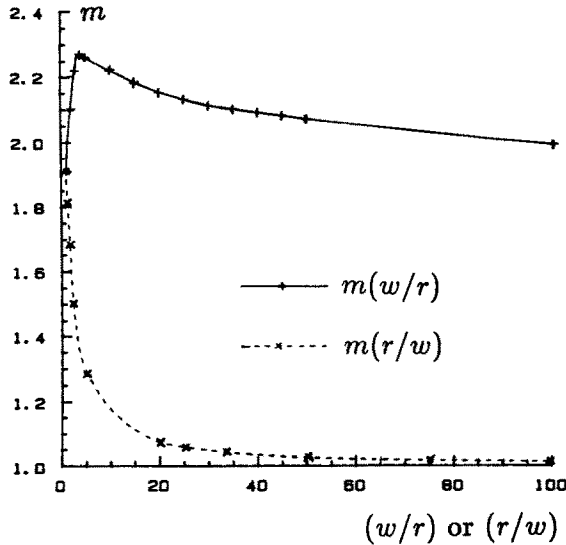


FIG. 11. m for a rectangular prismatic dislocation loop versus aspect ratio, measured as (r/w) or (w/r) , where r and $2w$ denote the loop dimensions perpendicular and parallel, respectively, to the crack front (see Fig. 3a). Symbols (+) (x) indicate discrete points at which equation (5.10) was integrated and from which the curves were constructed.

$$2(w+r)A_0 \ln m = \int_0^r \int_{-w}^{+w} -\frac{1}{2} b[\sigma_{yy}(x, 0, z) - \sigma_{yy}^{\text{full loop}}(x, 0, z)] dz dx. \quad (5.10)$$

Care must be taken to properly integrate equation (5.10) numerically, as there are integrable singularities involved in what is in principle an integration over four variables.

The results for m as a function of aspect ratio are presented in Fig. 11. Two different branches for m are shown, one corresponding to m for $r/w \geq 1$ and the other for $w/r \geq 1$. Two limits are clearly shown: for the case where $w/r \rightarrow \infty$, $m \rightarrow 2$ and $r/w \rightarrow \infty$, $m \rightarrow 1$. The former limit corresponds to the 2D geometry of a straight dislocation line oriented parallel to the crack front, which is analyzed in the following section. The latter limit corresponds to a rectangular loop of infinitely long dimension perpendicular to the crack front. It is only in this limit that $m = 1$, so that the elastic energy of the crack tip loop is given exactly by half that for the full loop representation. Although $m = 2$ rather than 1 for the 2D limit, RICE and THOMSON (1974) have shown that the full loop representation, which in this case is two infinitely long parallel dislocations of opposite sign separated by distance $2r$ in an uncracked infinite body, exactly produces the force acting in the x direction on the crack tip dislocation.

Certain features of Fig. 11 appear to be artifacts of the particular definition of m stated in equation (5.10). One such feature is the maximum for m which exists at approximately $w/r = 4$. The difference in energy, $2(w+r)A_0 \ln m$, between that for the crack tip dislocation loop and half that of the corresponding full loop representation is found instead to be a monotonically increasing function of w/r for loops of constant

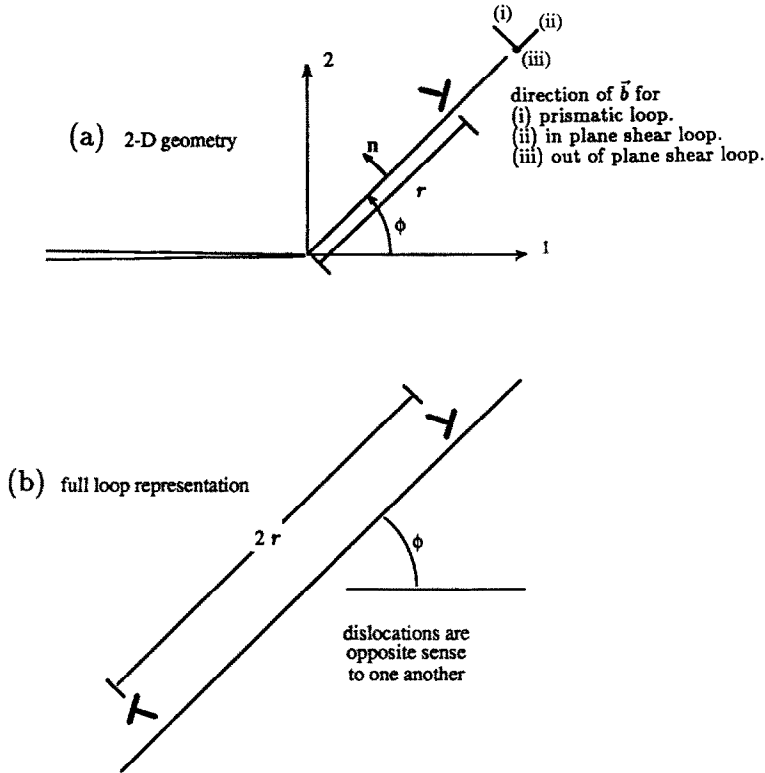


FIG. 12. (a) 2D crack-dislocation line geometry, and (b) full loop construction.

area $2wr$. Another feature is the difference in $m \approx 2.21$ for a semicircular loop compared to $m \approx 1.92$ for a rectangular loop with $r = w$. In fact, the difference in energies, $\pi r A_0 \ln m$ defined in equation (5.6) for the semicircular geometry and $4r A_0 \ln m$ defined in equation (5.6) for the rectangular case $r = w$, are within 5% of one another.

6. CALCULATIONS OF CORRECTION FACTOR m FOR 2D CRACK GEOMETRIES

3D calculations for shear dislocations and arbitrary orientations are complicated, and in order to cast the m values obtained for the prismatic loop into proper perspective, m is calculated here for a 2D crack tip dislocation line geometry as shown in Fig. 12a. The slip plane is oriented at angle ϕ to the crack plane, and components of \mathbf{b} are oriented either (i) perpendicular to the slip plane (prismatic), or in a shear loop mode for which components of \mathbf{b} may be (ii) perpendicular (edge, or in-plane, shear) or (iii) parallel (screw, or antiplane, shear) to the crack front.

Analytic function solutions as summarized by LIN and THOMSON (1986) for such 2D problems allow determination of the stress field $\sigma_{ij}(x, z)$ for the crack tip dislocation geometry shown in Fig. 12a, in which a straight dislocation line is parallel to and positioned at distance r from the crack front. The "full loop" geometry (now the loops are infinitely long in the z direction) is depicted in Fig. 12b as two straight

parallel dislocations of opposite sign to one another and separated by distance $2r$. In a manner similar to that for the semicircular and rectangular loop shapes, the energy \hat{U} per unit length of crack tip dislocation is defined in terms of one-half that for the full loop construction, plus the correction term,

$$\hat{U} = b_i A_{ij} b_j \ln \frac{2r}{r_0} + b_i A_{ij} b_j \ln m, \tag{6.1}$$

where $b_i A_{ij} b_j$ is the prelogarithmic energy factor for the crack tip dislocation, and r_0 is a core cut-off. RICE and THOMSON (1974), ASARO (1975) and RICE (1985c), in analyses of increasing generality, have noted that the radial force $d\hat{U}/dr$ attracting such a dislocation to the tip is $b_\alpha A_{\alpha\beta} b_\beta / r$. This is consistent with \hat{U} as in equation (6.1) for arbitrary m and confirms only that the prelogarithmic factor, but not the entire energy expression, is compatible with the approximation of writing the energy for a crack tip loop as half the full loop energy. Although the force, dU/dr , on a 2D straight dislocation line is unaffected by m , such is not the case for the 3D loop. Analogous to the 3D geometries discussed, we calculate m by

$$-\frac{b_j}{2} \int_0^r n_i [\sigma_{ij}(\rho, r, \phi) - \sigma_{ij}^{\text{full loop}}(\rho, r)] d\rho = b_i A_{ij} b_j \ln m, \tag{6.2}$$

where we note

$$\frac{1}{2} \sigma_{ij}^{\text{full loop}}(\rho, r) n_i b_j = \frac{b_i A_{ij} b_j}{r} \left[\frac{1}{1-\rho/r} + \frac{1}{1+\rho/r} \right]. \tag{6.3}$$

For the crack tip dislocation geometry, we define the stress field in isotropic solids in terms of three analytic functions of $\zeta = x_1 + ix_2 (= x + iy)$,

$$\begin{aligned} \sigma_{11} + \sigma_{22} &= 2\{\varphi'(\zeta) + \overline{\varphi'(\zeta)}\}, \\ \sigma_{22} - i\sigma_{12} &= \varphi'(\zeta) + \overline{\omega'(\zeta)} + (\zeta - \bar{\zeta})\overline{\varphi''(\zeta)}, \\ \sigma_{32} + i\sigma_{31} &= 2\eta'(\zeta), \end{aligned} \tag{6.4}$$

where

$$\begin{aligned} \varphi'(\zeta) &= \frac{A_e}{2b_e} B \left[\frac{1}{\zeta - \xi} \left(\sqrt{\frac{\xi}{\zeta}} + 1 \right) + \frac{1}{\zeta - \bar{\xi}} \left(\sqrt{\frac{\bar{\xi}}{\zeta}} - 1 \right) \right] \\ &\quad + \frac{A_e}{2b_e} \bar{B} \frac{\xi - \bar{\xi}}{2(\zeta - \bar{\xi})^2} \left[\sqrt{\frac{\xi}{\zeta}} + \sqrt{\frac{\zeta}{\bar{\xi}}} - 2 \right], \\ \eta'(\zeta) &= \frac{A_s}{2b_s} \left[\frac{1}{\zeta - \xi} \left(\sqrt{\frac{\xi}{\zeta}} + 1 \right) + \frac{1}{\zeta - \bar{\xi}} \left(\sqrt{\frac{\bar{\xi}}{\zeta}} - 1 \right) \right], \\ \omega'(\zeta) &= (\varphi')^* - (\varphi'_0)^* + \omega'_0 \end{aligned} \tag{6.5}$$

and where

$$\varphi'_0 = \frac{A_e}{b_e} B \frac{1}{\zeta - \xi}, \quad \omega'_0 = \frac{A_e}{b_e} \left[B \frac{1}{\zeta - \xi} - \bar{B} \frac{\xi - \bar{\xi}}{(\zeta - \bar{\xi})^2} \right].$$

The position of the dislocation for the geometry considered here is given by $\zeta = r \exp(i\phi)$, and the observation point along the slip plane by $\xi = \rho \exp(i\phi)$. A_e and A_s denote the prelogarithmic energy factor, $b_i A_{ij} b_j$, as calculated from either the edge or screw components, b_e or b_s of the Burgers vector, so that $A_e = \mu b_e^2 / 4\pi(1-\nu)$ and $A_s = \mu b_s^2 / 4\pi$. B is a complex number given by $-ie^{i\gamma}$ where $\gamma = \arctan(b_2/b_1)$. Here the notation $(\varphi'(\zeta))^* = \overline{\varphi'(\bar{\zeta})}$ is used.

The integrand in equation (6.2) is simply expressed for the three cases discussed here. For the (i) prismatic loop, $B = \exp(i\phi)$ and $\eta' = 0$; for (ii) in plane shear, $B = -i \exp(i\phi)$ and $\eta' = 0$, and for (iii) out of plane shear, $B = 0$ and $\varphi' = \omega' = 0$. Using these results with equations (6.2) and (6.3), the integrand becomes

$$\begin{aligned} & \frac{1}{2} n_i [\sigma_{ij}(\zeta = \rho e^{i\phi}, \xi = r e^{i\phi}) - \sigma_{ij}^{\text{full loop}}(\rho)] b_j \\ &= \frac{A_e}{r} \left[\frac{b_e r}{2A_e} \Re \{ (\varphi' + \overline{\omega'} + (\zeta - \bar{\zeta}) \overline{\varphi''}) e^{-2i\phi} + 4\varphi' \sin^2 \phi \} - \left(\frac{1}{1-\rho/r} + \frac{1}{1+\rho/r} \right) \right] \\ & \hspace{15em} \text{(i) prismatic,} \\ &= \frac{A_e}{r} \left[\frac{b_e r}{2A_e} \Re \{ (\varphi' + \overline{\omega'} + (\zeta - \bar{\zeta}) \overline{\varphi''}) i e^{-2i\phi} - 2\varphi' \sin 2\phi \} - \left(\frac{1}{1-\rho/r} + \frac{1}{1+\rho/r} \right) \right] \\ & \hspace{15em} \text{(ii) in plane shear,} \\ &= \frac{A_s}{r} \left[\frac{b_s r}{A_s} \Re \{ \eta' e^{i\phi} \} - \left(\frac{1}{1-\rho/r} + \frac{1}{1+\rho/r} \right) \right] \quad \text{(iii) out of plane shear,} \quad (6.6) \end{aligned}$$

where each expression in square brackets defines a dimensionless function of ρ/r and angle ϕ . Presented in Figs. 13, 14, and 15 are the differences, $-(1/2)(\sigma_{ij} - \sigma_{ij}^{\text{full loop}}) n_i b_j$, for the prismatic, in plane shear, and out of plane shear loops, respectively, as functions of position, ρ/r , within the loop and angle ϕ . This difference represents the integrand in equation (6.2) for the energy change between the approximate half-full-loop and exact representations for a crack tip dislocation loop. The profiles show as functions of position, ρ/r , the additional (if the abscissa is positive) elastic work performed in forming the dislocation loop at the crack tip as opposed to forming a full dislocation loop in an infinite, uncracked body. Three slip plane angles, $\phi = 0, 45^\circ$, and 90° are chosen for profiles in each type of loop. In all cases, the largest energy difference occurs when the loop and slip planes are coplanar ($\phi = 0$), and it diminishes as ϕ increases to 90° . As in the study of the prismatic 3D loops in Section 5, the sign of the profiles for $\phi = 0$ are positive for all ρ/r .

In all cases, there is an inverse square root singularity in the abscissa as $\rho = 0$ is approached. As $\rho/r \rightarrow 1$, the abscissa goes to zero, signifying that the approximate half-full-loop energy representation exactly characterizes the image force exerted on the dislocation in the presence of the crack.

The resulting correction factors m for the prismatic and shear loops are presented in Fig. 16. For all three types of loops, m is the largest and equals 2 at $\phi = 0$, and monotonically decreases through to $\phi = 90^\circ$. This suggests that the estimate of

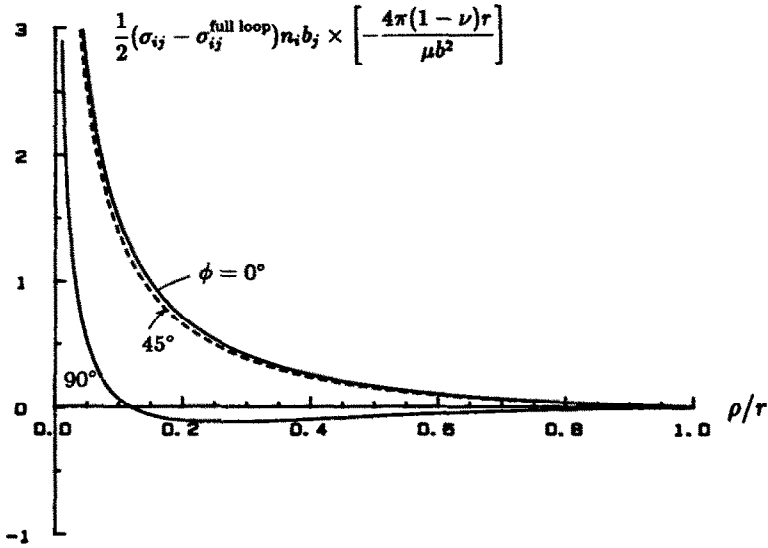


FIG. 13. Stress difference, 2D prismatic loop.

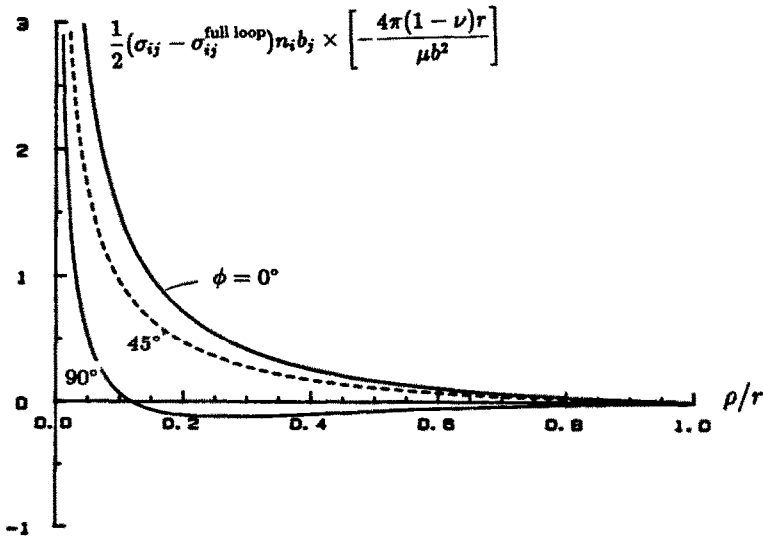


FIG. 14. Stress difference, 2D in plane shear loop.

$m = 2.21$ for the prismatic semicircular loop is an upper bound to m for the semicircular geometry. Although the endpoint values of m for the prismatic and in-plane shear loops are identical, m for the latter type of loop decays much more rapidly with ϕ than for the former. In this 2D geometry, unlike the semicircular loop or other 3D

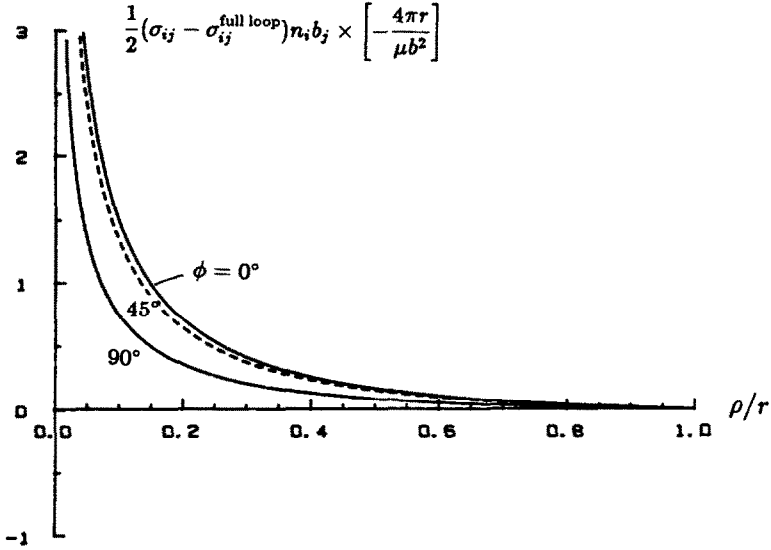


FIG. 15. Stress difference, 2D out of plane shear loop.

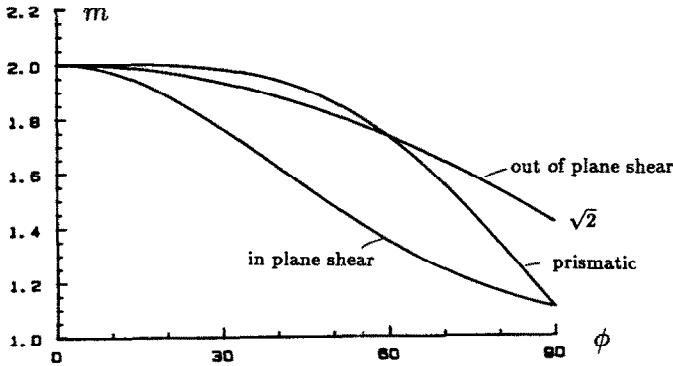


FIG. 16. Correction values, m , for 2D loops.

geometry, a value of m other than unity does not affect the image force exerted on the dislocation, as may be seen by differentiating $\hat{U}(r)$ in equation (6.1).

The implications of the 2D study here and the 3D study in Section 5 in regard to the choice of m for general 3D loop geometries is discussed next.

7. ESTIMATE OF m FOR A GENERAL 3D SHEAR DISLOCATION LOOP

In principle, analogous procedures to that presented here for the coplanar prismatic dislocation loop may be used to calculate m for general loop shapes, with arbitrary slip plane and Burgers vector orientations. Since such 3D calculations are complicated,

an approximate procedure to estimate m in such cases is proposed, based on knowledge of m for the identically shaped prismatic loop situated on the crack plane ahead of the crack, and an understanding of how the analogously defined m for the 2D "loop" varies with slip plane and Burgers vector orientations. In general, $m = m(\phi, \psi, s)$, where ϕ measures the angle subtended by the uncracked extension of the crack and slip planes, ψ measures orientation of the Burgers vector, and s denotes the variable(s) to describe the loop shape (e.g. r/w for a rectangular loop).

The approximation made is to estimate the dependence of m^{3D} on loop shape by comparing the 3D and analogously defined 2D values of m for the particular case addressed earlier, of a prismatic loop situated on the crack plane ahead of the crack ($\phi = 0$). The dependence of m^{3D} on slip plane and Burgers vector is assumed to be that for the 2D case. In particular, it is proposed that

$$\ln m^{3D}(\phi, \psi, s) \approx \frac{\ln m^{3D}(\phi = 0, \text{prismatic}, s)}{\ln m^{2D}(\phi = 0)} \ln m^{2D}(\phi, \psi). \quad (7.1)$$

Thus, this approximation has the feature that $m^{3D}(\phi = 0)$, like $m^{2D}(\phi = 0)$, is independent of ψ . [Added note: This feature is incompatible with recent calculations made by GAO and RICE (1987), following preparation of this manuscript which determine $m^{3D}(\phi = 0)$ for a semicircular shear loop to vary from 2.67 when \mathbf{b} is perpendicular to the crack front to 1.99 when \mathbf{b} is parallel to the crack front. For comparison, the value given here is 2.21 for a prismatic loop.]

For a general shear loop, $m^{2D}(\phi, \psi)$ can be written using calculated values of m_e^{2D} (edge, in plane shear) and m_s^{2D} (screw, out of plane shear) provided in Fig. 16

$$[A_e(\psi) + A_s(\psi)] \ln m^{2D}(\phi, \psi) = A_e(\psi) \ln m_e^{2D}(\phi) + A_s(\psi) \ln m_s^{2D}(\phi), \quad (7.2)$$

where $A_e = \mu b_e^2 / 4\pi(1 - \nu)$, $A_s = \mu b_s^2 / 4\pi$ are the prelogarithmic energy factors associated with the edge and screw components, b_e and b_s , of the Burgers vector.

This approximate method was used to estimate m for studies of crack tip nucleation of full and partial dislocation loops with semicircular shape by ANDERSON (1986). For example, for f.c.c. geometries in which the crack front lies along $\langle 110 \rangle$, the three full and three partial Burgers vectors on a $\{111\}$ slip plane are oriented at angles $\psi = 30^\circ$, 90° and $\psi = 0, 60^\circ$, respectively, to a reference line normal to the crack front and in the slip plane. Using equations (7.1), (7.2), and noting that $m^{3D} \approx 2.21$ for the prismatic semicircular loop oriented at $\phi = 0$, we obtain the approximation

$$\ln m^{3D}(\phi, \psi) \approx \frac{\ln 2.21}{\ln 2} \left[\frac{\cos^2 \psi \ln m_e^{2D}(\phi) + (1 - \nu) \sin^2 \psi \ln m_s^{2D}(\phi)}{\cos^2 \psi + (1 - \nu) \sin^2 \psi} \right] \quad (7.3)$$

where $\ln m_e^{2D}(\phi)$ and $\ln m_s^{2D}(\phi)$ are used from Fig. 16.

Figure 17 shows estimates of m for the semicircular loop for the four values of ψ mentioned, as a function of slip plane angle ϕ , using $\nu = 0.3$ as a typical value for many metals. The general features are that m here as in the 2D case is independent of ψ when $\phi = 0$, and that as ϕ increases, m is ordered from lowest to highest as ψ changes from 90° (i.e., with Burgers vector parallel to the crack front) to 0° (i.e., with Burgers vector perpendicular to the crack front). [Added note: As mentioned, the

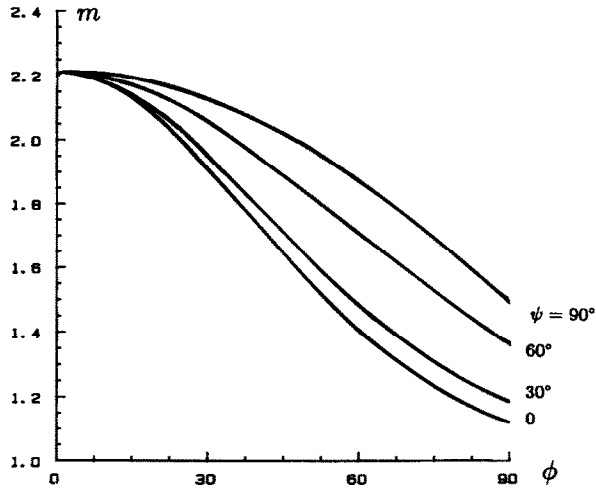


FIG. 17. Estimates of m for a semicircular shear loop as a function of slip plane angle ϕ to the uncracked extension of the crack plane and Burgers vector orientation ψ , where $\psi = 0^\circ$ and 90° describe shear Burgers vectors perpendicular and parallel, respectively, to the crack front.

former feature is incompatible with recent extensions of the 3D calculation, outlined in Section 5.2, to the shear loop case.]

In applications to tensile loaded cracks with tips along $\langle 110 \rangle$ in f.c.c. crystals or along interfaces between crystals (ANDERSON, 1986), consideration of representative ranges of ϕ at which the most highly stressed $\{111\}$ planes lie, and of the ψ values appropriate to the full and partial dislocation Burgers vectors activated by such loading, suggests a practical range of m for semicircular shear loops between approximately $m = 1.2$ and 1.9 . Since the critical applied K_1 predicted to make such a loop grow unstably scales with $1/\sqrt{r_0}$ (MASON, 1979; ANDERSON and RICE, 1986), and since the effect of m is to replace r_0 by r_0/m , K_1 for dislocation nucleation scales as \sqrt{m} . Thus, inclusion of the m correction causes a representative increase in the predicted K_1 for nucleation by 10 to 40%.

ACKNOWLEDGEMENTS

This study was supported by the NSF Materials Research Laboratory at Harvard University, under grant NSF-DMR-83-16979 and by the ONR Mechanics Division, contract N00014-85-K-0405 with Harvard University. Final results for some of the numerical integrations were obtained through the Cambridge University Phoenix Computing Facility.

REFERENCES

- ANDERSON, P. M. 1986 *Ductile and Brittle Crack Tip Response*, Ph.D. Thesis, Harvard University, Cambridge, MA, U.S.A.

- ANDERSON, P. M. and RICE, J. R. 1986 *Scripta Metall.* **20**, 1467.
 ASARO, R. J. 1975 *J. Phys. F: Metal Phys.* **5**, 2249.
 BACON, D. J., BARNETT, D. M. 1979 *Prog. Mater. Sci.* **23**, 51.
 and SCATTERGOOD, R. O.
 BARNETT, D. M. and ASARO, R. J. 1972 *J. Mech. Phys. Solids* **20**, 353.
 BUECKNER, H. F. 1987 *Int. J. Solids Struct.* **23**, 57.
 BUECKNER, H. F. 1977 in *Fracture Mechanics and Technology*, Vol. 2,
 (edited by G. C. SIH and C. L. CHOW), p.
 1069. Sijthoff and Noordhoff, Amsterdam.
- GAO, H. and RICE, J. R. 1987 research in progress.
 HIRTH, J. P. and LOTHE, J. 1968 *Theory of Dislocations*. McGraw-Hill, New York.
 LIN, I. H. and THOMSON, R. 1986 *Acta Metall.* **34**, 187.
 MASON, D. D. 1979 *Phil. Mag.* **39**, 455.
 OHR, S. M. 1985 *Mat. Sci. Eng.* **72**, 1.
 RICE, J. R. 1985a *J. Appl. Mech.* **52**, 3.
 RICE, J. R. 1985b *Int. J. Solids Struct.* **21**, 781.
 RICE, J. R. 1985c in *Fundamentals of Deformation and Fracture*, J.
 D. Elshelby Memorial Symposium (edited by
 B. A. BILBY, K. J. MILLER and J. R. WILLIS), p.
 33. Cambridge University Press, Cambridge.
- RICE, J. R. and THOMSON R. 1974 *Phil. Mag.* **29**, 73.
 SCATTERGOOD, R. O. 1980 *Acta Metall.* **28**, 1703.
 STROH, A. N. 1958 *Phil. Mag.* **3**, 625.